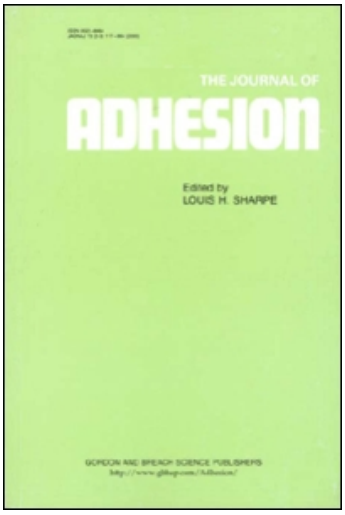

The Journal of Adhesion
Publication details, including instructions for authors and subscription information:
http://www.informaworld.com/smpp/title~content=t713453635

An Assessment of Carbon Fiber/Organic Matrix Interactions

L. H. Peebles Jr.[a]
[a] Chemistry Division, Naval Research Laboratory, Washington, DC, USA

To cite this Article Peebles Jr., L. H.(1995) 'An Assessment of Carbon Fiber/Organic Matrix Interactions', The Journal of Adhesion, 54: 1, 1 — 22
To link to this Article: DOI: 10.1080/00218469508014377
URL: http://dx.doi.org/10.1080/00218469508014377

J. Adhesion, 1995, Vol. 54, pp. 1–22
Reprints available directly from the publisher
Photocopying permitted by license only

An Assessment of Carbon Fiber/Organic Matrix Interactions*

L. H. PEEBLES, Jr

Chemistry Division, Naval Research Laboratory, Washington, DC 20375-5342, USA

(Received April 23, 1994; in final form June 10, 1994)

The various mechanisms of adhesive bonding of carbon fibers to organic matrices are reviewed. These mechanisms include covalent bonding, acid-base interactions, residual compressive stresses which result from fabrication procedures and mechanical interactions. Because elimination of oxygen groups by heat treatment or by reacting surface oxygen groups with blocking agents has little effect on the interfacial shear strength (reductions of 10–30%), covalent bonding is not the dominant mechanism. Acid-base and residual compressive stresses do not explain differences observed in the interfacial shear strength in thermoplastic resins that contain carbon fibers with similar surface chemistry. The new method of scanning tunneling microscopy provides evidence that mechanical interactions with surface microroughness may possibly be the most important mechanism of adhesion. However, at present, techiques to quantify microroughness and thereby relate to interfacial shear strength are only now being developed.

KEY WORDS AND PHRASES Covalent bonding; acid-base interactions; residual compressive stresses; mechanical interactions; microroughness; interlaminar shear strength; interfacial shear strength; blocking of active sites.

INTRODUCTION

Differences of opinion exist regarding the primary type of interaction between carbon fibers and organic matrices. The interactions include covalent bonding, acid-base interactions (a term intended to include hydrogen bonding, dipolar, columbic, and other "low energy" interactions), compressive forces owing to shrinkage of the matrix from the molding or cure state, and mechanical interactions with surface rugosity. The purpose of this paper is to review the evidence for these interactions.

The usual methods of ascertaining fiber/matrix interactions include measuring the interfacial shear strength (IFSS) on model composites or the interlaminar shear strength (ILSS) on high-volume-fraction composites. The IFSS can be determined by the various methods indicated in Figure 1:[1] fiber pull-out, fiber push-out, fiber fragmentation and microdrop fracture. The advantages and disadvantages of these methods have been summarized.[2,3] The ILSS can be determined from high-volume-fraction fiber composites such as those indicated in Figure 2.[2]

* One of a Collection of papers honoring James P. Wightman, who received the 13th Adhesive and Sealant Council Award at the ASC's 1993 Fall Convention in St. Louis, Missouri, USA, in October 1993.

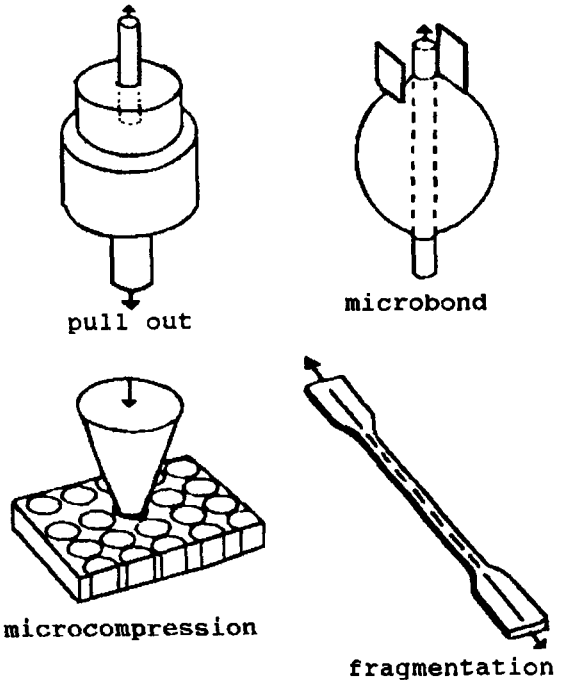

FIGURE 1 Methods currently used for measuring the interfacial shear strength (IFSS) of the fiber/matrix interface (Piggott[1], © Elsevier Science Publishers BV, Academic Publishing Division, reprinted with permission).

SURFACE ANALYTICAL TECHNIQUES

If reactive groups are constrained to the surface of a fiber and occupy an area, a, of $1\,nm^2$, then a fiber with a density, ρ, of $1.8\,g/cm^3$ and a diameter, d, of $7\mu m$ and a perfectly smooth circular perimeter would contain $4/\rho d a N_A = 5.3 \times 10^{-7}$ moles/gram of reactant groups, where N_A is Avogadro's number. This low concentration is to be contrasted with a stoichiometric mixture of the diglycidylether of bisphenol A (DGEBA) and meta-phenylenediamine (m-PDA) which contains 4.5×10^{-3} moles/gram of epoxy groups. The low concentration of surface groups makes them difficult to identify and to quantify. Usual techniques include titration, reaction of surface groups with more easily identifiable tags, x-ray photoelectron spectroscopy (XPS, also known as electron spectroscopy for chemical analysis ESCA), Auger spectroscopy, secondary ion mass spectroscopy (SIMS), infrared spectroscopy, Raman spectroscopy, surface energy through wetting experiments, inverse gas chromatography, surface area and pore structure by gas or liquid adsorption, and scanning tunneling microscopy to obtain information on surface rugosity. Figure 3 provides a schematic diagram of how some of these techniques probe the volume near the surface.[4] The reaction of surface groups with tagged molecules is also limited to a very thin surface layer. The calculation given above assumes a uniform distribution of surface active groups. Examination of the surface of both mesophase- and PAN-based carbon

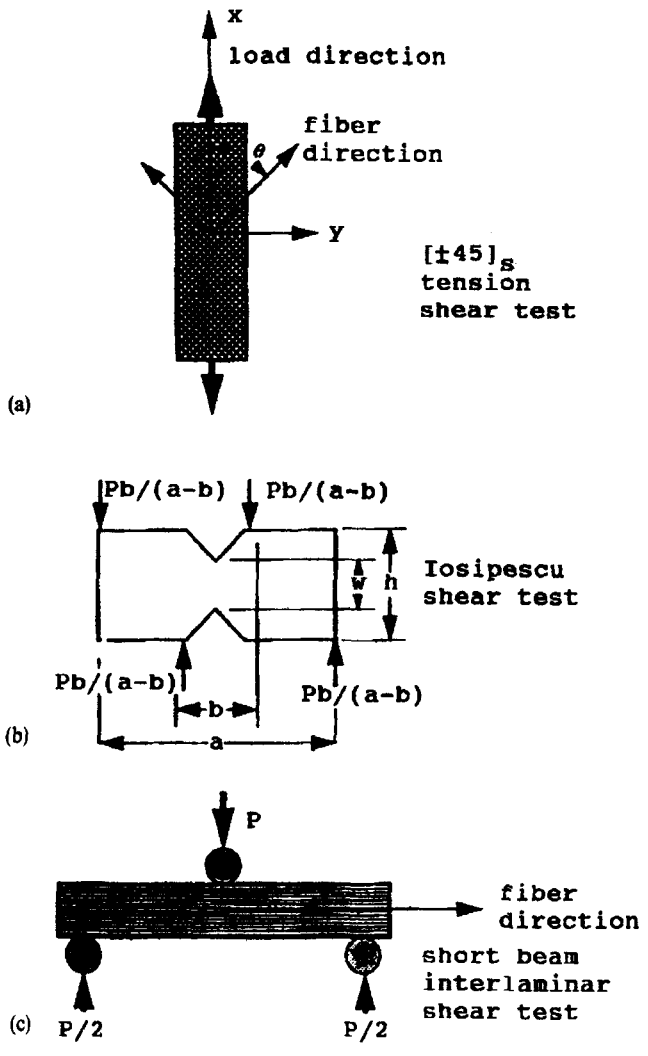

FIGURE 2 Schematic representation of composite interlaminar shear strength tests (ILSS): a) [±45], tension shear test; b) Iosipescu shear test; c) short beam interlaminar shear test (Herrera-Franco and Drzal[2], reprinted by permission of the publishers, Butterworth Heinemann Ltd,©)

fibers by the scanning Auger microscope shows that the formation of oxygen species varied widely on both untreated and treated fibers within the region of observation, along a filament, and between filaments on fibers. Figure 4 shows the non-uniform oxygen distribution on an oxidized Tonin mesophase-based carbon fiber (oxidized in 60% nitric acid at reflux for 24 hr) as islands of oxygen atoms[5]. This figure and others in the article demonstrate the non-homogeneous composition of the fiber surface.

XPS has been used to identify chemical groups at or near the fiber surface. As shown in Figure 3, XPS probes well below the surface of the fiber. The total concentration of

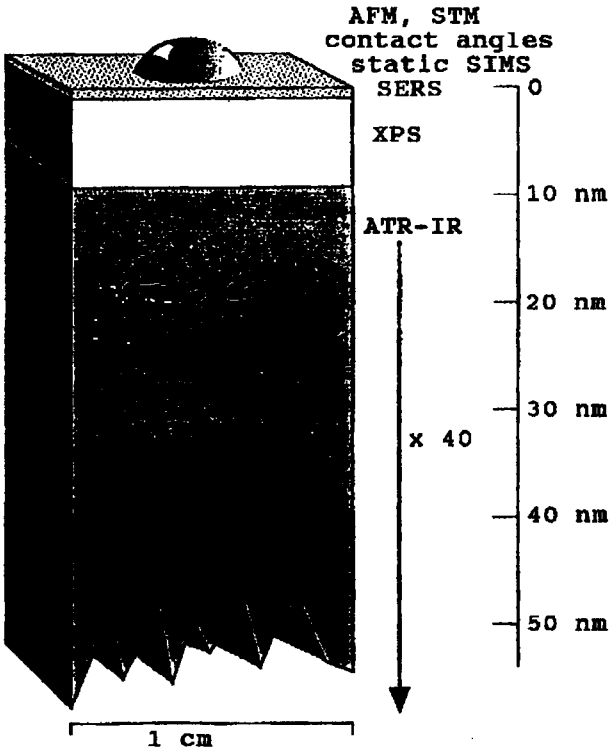

FIGURE 3 The major surface analytical techniques probe to different depths. Contact angles, scanning tunneling microscopy (STM), atomic force microscopy (AFM) and static secondary ion mass spectroscopy (SIMS) are extremely surface localized. (Reprinted by permission of the publisher from Ratner[4],© 1993 by Elsevier Science Publishing Co., Inc.).

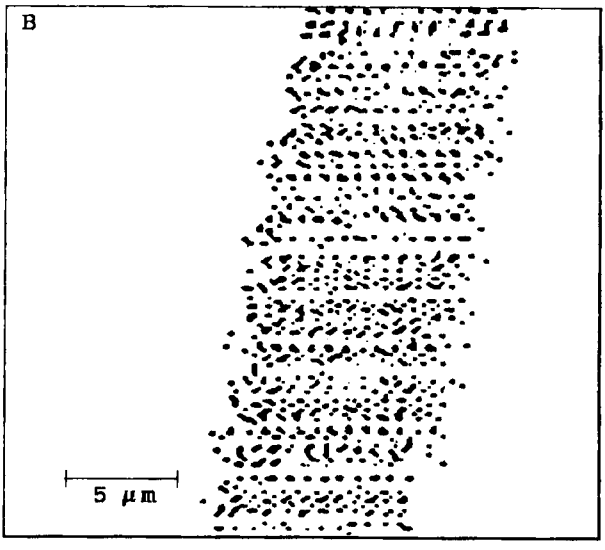

FIGURE 4 Scanning Auger microscope distribution of oxygen on an oxidized Tonin mesophase-based carbon fiber containing ~14.3% oxygen, as determined by XPS (Lin[5]).

chemical groups detected by XPS will depend upon 1) the take-off angle used to collect the data (the x-ray beam penetrates different depths into the fiber depending on the angle of incidence) 2) the curve resolving scheme and 3) the sample used for calibrating intensities. As the crystal structure of the carbon fiber surfaces can vary from turbostratic to graphitic, this variation will affect the shape of the C_{1s} band and, thus, selection of the proper shape will influence concentrations based on the deconvolution[6], see Table I.

To gain information on the reactivity of groups identified by XPS as being present at or near the surface, various model compounds can be reacted with the surface that are specific to certain groups and also contain tags that have very high XPS signals. Trifluoroacetic anhydride reacts with carboxyl and hydroxyl groups,[7] trifluoroethanol can be reacted with carboxyl groups[7], trifluorophenylhydrazine,[7] pentafluorophenylhydrazine[8] or pentafluorobenzyl bromide[9] with carbonyl groups, a fluorinated cholorosilane with hydroxyl groups,[9] and pentafluorobenzaldehyde with primary amine groups.[6] Some of these reactions can be conducted with the additive in solution or in the gaseous phase. The amount of olefinic bonds can be estimated by reaction with mercuric trifluoroacetate.[8] Thallium (II) ethoxide will react with acid groups with pK_a's less than 20. The metal is rare in nature, is not expected to exist in commercial fibers, and has a very strong XPS signal.[10] The total oxygen and the reactive surface groups determined by these analytical techniques are given in Table II.

The low reactivity of "surface" oxygen as determined by XPS is also apparent when comparison is made between either the concentration of total oxygen or carbonyl oxygen with IFSS when a variety of different surface treatment techniques are used, Figure 5 and Figure 6.[11] On the contrary, an excellent correlation was found between ILSS and oxygen content determined by XPS on a series of PAN-based carbon fibers that differed only in the extent of anodic oxidation, Figure 7. The difference between these two sets of figures can be ascribed to the different methods of introducing oxygen groups onto fiber surfaces used for the samples of Figure 5 and Figure 6, while the mechanisms controlling ILSS in Figure 7 and introducing oxygen moieties were consistently altered by use of the same surface treatment, only varying the extent of treatment. A closer look at Figure 5 shows that lower ratios of O_{1s}/C_{1s} fairly high values of ILSS are obtained. Drzal *et al.*[12] examined a series of Hercules IM-6 fibers which had received 0, 20, 100, 200 and 600% of their commercial surface treatment. The IFSS showed a linear increase with increasing O/C ratio (recalculated from their data) in the region 0.02 to 0.20. On the other hand, ILSS determined by the short beam shear

TABLE I

The percentage of functional group, relative to carbon for oxidized Torayca T-800-H carbon fibers analyzed by two different models for the C_{1s} shape (after Nakayama *et al.*[6]).

Oxidized Model	−COOH	−COOR	>C=O	C−OH	Other
Weakly graphitic	0.2	0.9	1.3	0.1	0.4
Strongly graphitic	1.5	2.6	5.1	0.3	3.1
Weakly aliphatic	0.2	4.0	5.4	0.1	10.7
Strongly aliphatic	1.5	5.6	9.2	0.3	12.5

Others include ether, C=N, or peroxides

TABLE II
Concentration of functional groups per hundred surface atoms, based on functional group derivatization and fluorine, mercury, or thallium XPS analysis

Fiber	Total oxygen	−OH	>C=O	−COOH	−NH	>C=C<	Tl	Ref
IM-7	14	0.7	1.1	1.8	nd	nd	nd	9
IM-8X	10.9	nd	nd	nd	nd	nd	1.10	10
T-650-42	11	0.5	1.4	1.6	nd	nd	nd	9
	10.6	nd	nd	nd	nd	nd	0.27	10
G-40-800	15	0.7	1.3	1.2	nd	nd	nd	9
T-40	2.7	0.2	1.8	0.6	nd	nd	nd	9
AS-4	11	0.1	0	0.4	1.0	1.8	nd	8
Celion 6000	14	0.2	0.2	0.3	0.6	0.4	nd	8
T-300	20	1.1	2.1	0.4	nd	nd	nd	7
T-300-6k	10.2	nd	nd	nd	nd	nd	1.75	10
T-300-12k	10.3	nd	nd	nd	nd	nd	1.81	10
Apollo 53	5	nd	nd	nd	nd	nd	0.33	10
Hitex fiber	10.2	nd	nd	nd	nd	nd	0.74	10

nd: not determined
Note: Thallium analysis has a coefficient of variation of 20%. The reported number is the average of three determinations.

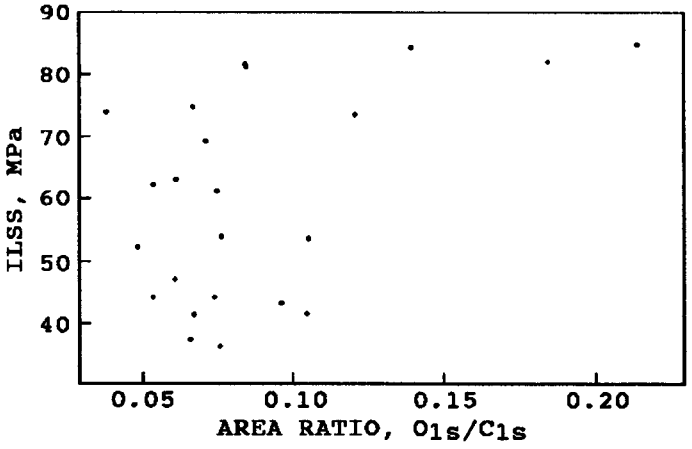

FIGURE 5 Variation in ILSS with O_{1s}/C_{1s} XPS area ratio for fibers anodically oxidized in various electrolytes (Reprinted with permission from Harvey *et al.*,[11] Figure 11,© Chapman & Hall, UK).

test showed essentially no increase beyond the 20% treatment level, a result similar to that shown in Figure 7. In the latter case, the shear strength of the composite may be *limited* by the shear strength of the matrix if it is assumed that the IFSS of the 20% surface treated fibers is close to the matrix shear strength.

It may be that incorporation of oxygen plays a minor role in effecting adhesion. In agreement with this postulate, the atomic percent of oxygen determined by XPS was some six times that of thallium on Amoco T-300 fibers anodically oxidized in HNO_3 as a function of treatment level followed by reaction with thallous ethoxide.[10]

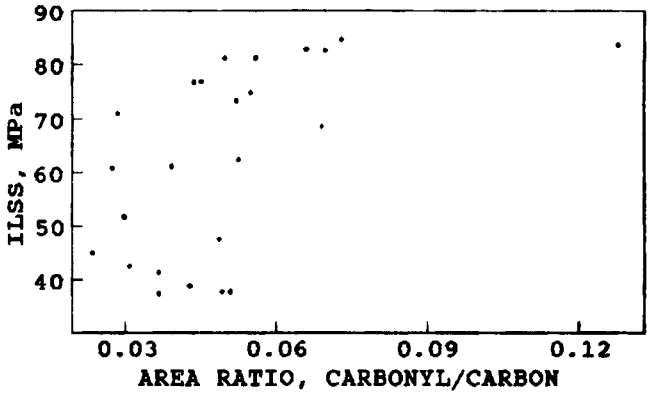

FIGURE 6 Variation of ILSS with carbonyl group /C_{1s} XPS area (represented by the ratio of the area of the C_{1s} peak due to carbonyl to that due to graphitic carbon) (Reprinted with permission from Harvey *et al.*,[11] Figure 12,© Chapman & Hall, UK).

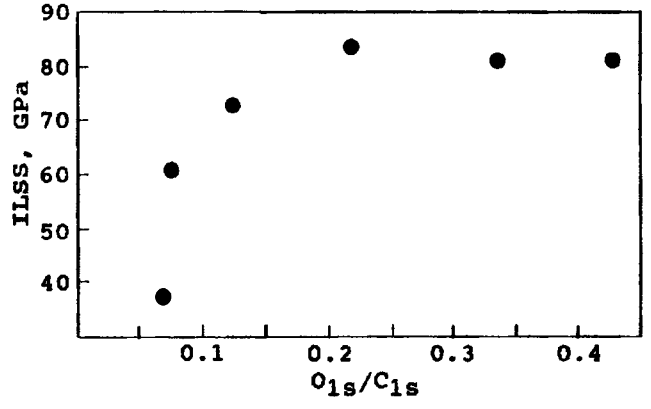

FIGURE 7 Variation of ILSS with O_{1s}/C_{1s} for potentiostatically-treated fibers in 0.5 M nitric acid. (Reprinted with permission from Harvey *et al.*,[11] Figure 11,© Chapman & Hall, UK).

COVALENT BONDING

Surface oxygen on carbon materials can be removed by heat treatment in vacuum at temperatures above 700 °C. Figure 8 shows that the ILSS of an anodically-oxidized, high-strength PAN-type fiber is augmented by heat treatment at 1000 °C prior to formation of the composite.[11] A similar result was obtained by examining some Hercules fibers that were not surface treated, surface treated by a proprietary method, and surface treated then heat treated at high temperature, Figure 9.[13] Two sets of authors suggest that exposing the heat-treated fiber to air at room temperature may result in the formation of non-acidic oxides, thereby resulting in improved adhesion over the untreated fiber.[11,14]

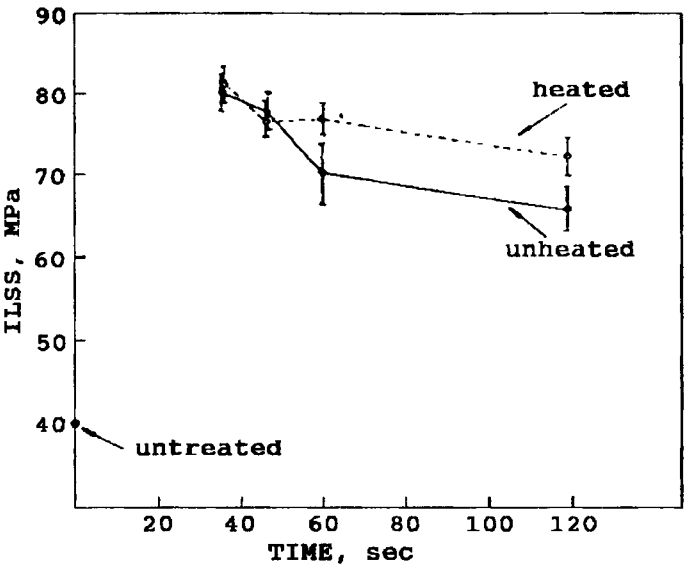

FIGURE 8 ILSS of fiber anodically oxidized in 0.5 M HNO_3 at 3.0 V for various times. Some samples heat treated at 1000°C in vacuum (Reprinted with Permission from Harvey *et al.*,[11] Figure 15,© Chapman & Hall, UK).

An attempt was made to differentiate the influence of various surface oxides on the ILSS of unidirectional composites by use of specific chemical blocking agents[15]. Carboxylic acid groups can be esterified with methanol, while both carboxyls and hydroxyls can be blocked with diazomethane, CH_2N_2. As the preparation of purified CH_2N_2 is a lengthy, difficult process, a simplified *in situ* procedure of placing carbon fibers into the CH_2N_2 generation reactor was also used. This latter procedure resulted in reactions with other polar surface groups in addition to carboxyls and hydroxyls, hence the reagent(s) are non-specific. It was used for a "total blocking of all reactive centers originating during the surface treatment procedure" (author's statement). Carbonyl and quinone groups can be blocked by reduction with $NaBH_4$ in alkaline solution followed by reaction with CH_2N_2. The results of such treatments are shown in Figure 10 for some (proprietary) surface-treated carbon fibers. Blocking of —COOH and —OH groups by purified CH_2N_2 resulted in a 24–30% reduction in ILSS, while treatment with the contaminated CH_2N_2 resulted in a 65–75% reduction. Whether the contaminated CH_2N_2 only reacted with active surface groups or had some other effect, such as modification of reaction rates or of the surface itself, is open to how one wishes to explain the results as the reaction of contaminated CH_2N_2 with known groups has not been demonstrated. The sharp decrease in ILSS is explained by assuming reaction with all active surface groups.

Reaction of non-surface-treated Sigrafil HT fibers with purified CH_2N_2 resulted in a 15% reduction in ILSS but no reduction in ILSS for non-surface-treated Sigrafil HM. These results indicate the presence of surface active groups on HT-type fibers and essentially no such groups on the HM-type fibers. The first three fibers in Figure 10 also

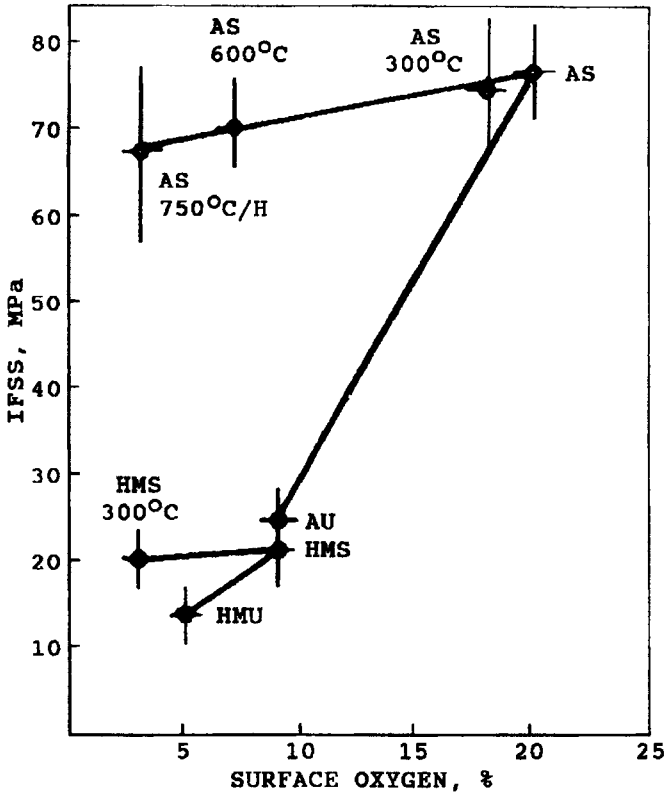

FIGURE 9 IFSS of a high modulus untreated (HMU) and surface treated (HMS) and a high strength untreated (AU) and surface treated (AS) as received and after the designated heat treatment under vacuum or hydrogen (Drzal *et al.*,[13] reprinted with permission from Gordon and Breach Science Publishers).

show reductions in ILSS when just the acid groups, the hydroxyl groups or the quinone/carbonyl groups are blocked, but significant amounts of ILSS remain. Unfortunately, the blocking reactions are difficult to effect and are time consuming (requiring days), hence the data could not be quantified to determine the effect of each type of surface active group. The main conclusion to be derived from this work is that covalent bonding, while present, is not the primary mechanism of adhesion. In an earlier paper, Fitzer and Weiss concluded that at least 50% of the adhesion improvement by fiber oxidation is of a pure chemical nature.[16]

Based on the diminution of the carboxyl area and the increase of the —C—O— area under the C_{1s} XPS peak on addition of a thin layer of resin, the conclusion was reached that there is definite evidence for chemical bonding between the oxidized fiber surface and a DGEBA resin.[17] The statement was made, however, that it was not possible to concluded whether chemical bonding was responsible for the increased interlaminar shear strength of composites produced from treated fibers. The high modulus fibers (more perfect graphitic surface structure) are less reactive towards oxidation than the high strength fibers. These authors also concluded that carboxyl and ester groups are

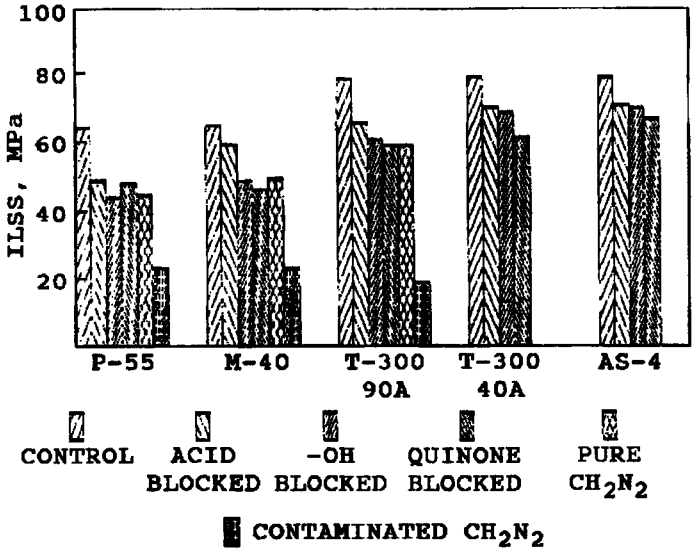

FIGURE 10 The effect of various blocking treatments on the ILSS of commercially surface treated high modulus and high strength fibers (after Fitzer and Weiss[15]).

formed at the edge sites of the carbon crystal, whereas keto-enol groups are formed on the basal planes. The oxygen-containing groups may be produced at different orientations and at different depths into the fiber. Incorporation of oxygen-containing groups deep within the fiber would preclude reaction with test molecules as indicated in Tables I and II.

Drzal[18] reacted the same series of IM-6 fibers with butyl glycidyl ether, a mono epoxide, prior to fabrication of IFSS specimens. The blocked specimens had IFSS values some 30% lower than those of the non-blocked specimens.

THERMOPLASTIC RESINS

The adhesion of carbon fibers to thermoplastic resins is generally low, with some exceptions. There are major differences between these two types of matrices: for thermoplastic matrices there are few if any reactive groups, their moduli are lower than thermosets, they fail by yielding rather than by brittle fracture, they are tougher than thermosets and the processing procedures are less favorable for total wetting.

The Cox equation for shear stress transfer from a matrix resin to an embedded fiber is[19]

$$\tau = E\varepsilon_m \left(\frac{G_m}{2E \ln\left(\frac{R_1}{r}\right)} \right)^{1/2} \frac{\sinh \beta(0.5L - x)}{\cosh\left(\beta \frac{L}{2}\right)} \tag{1}$$

where ε_m is the strain in the matrix; G_m, shear modulus of the matrix; R_1, interfiber spacing; r, fiber radius; ß, a scaling factor; L, length of fiber fragment; x, radial distance outward; τ, interfacial shear strength at a fixed point. Given that all other parameters are constant, the equation predicts that the interfacial shear stress depends on the square root of the matrix shear modulus times the strain, $G_m^{1/2}\varepsilon_m$. The matrix shear modulus is lower in thermoplastics than in thermosets. Also, the thermoplastics have extremely high viscosity relative to the more monomeric thermosets, there is a molecular weight distribution which may segregate at the interface, and they are extremely process sensitive (*i.e.* use and elimination of casting solvents, variations in glass transition temperatures, temperature history, crystallinity, etc.). However, some fibers do adhere well to both matrix types while other fibers adhere well to epoxies but not to thermoplastics. The reasons for these differences are not understood.[20,21] SEM photographs of failed epoxy and other thermosetting resins show that the fibers are coated with resin while similar photographs of failed thermoplastic composites indicate that the fibers separated cleanly from the matrix. It is possible that a thin layer of thermoplastic resin remains on the fibers, but the differences in the photographs strongly indicate differences in fiber-matrix adhesion.

The critical aspect ratio is defined as l_c/d from the Kelly-Tyson equation[22]

$$\tau = (\sigma_f/2)(d/l_c) \tag{2}$$

where τ is the interfacial shear strength; σ_f, the fiber tensile strength at the critical length l_c; and d the fiber diameter. This ratio is inversely proportional to τ provided that σ_c is not affected by surface treatment and is similar for fibers of different manufacture and surface treatment (see Appendix for a comparison of σ_c among these fibers). Critical aspect ratios for Hercules AS-1 and AS-4 fibers and Hysol Grafil XAS fiber in an epoxy resin are given in Table III. Also in Table III are these same fibers as well as Hercules AU-4 in several thermoplastic resins. While there are discrepancies in the table for measurements in the same resin but at different laboratories, such discrepancies are not unusual. In a round-robin examination of the single filament fragmentation test among seven laboratories, IFSS varied from 29 to 69 MPa with an average of 47.3 Mpa.[23] In all cases, the increase in critical aspect ratio in Table III between the epoxy and the thermoplastics demonstrates lower adhesion to the thermoplastics, but there is a significant difference between the AS-type fibers and XAS, the last having an enhanced

TABLE III
Critical aspect ratio for carbon fibers in thermosetting and thermoplastic matrices

Matrix	AS-1	AU-4	AS-4	XAS	Ref
DGEBA/*m*-PDA	42		55	32	21
Polycarbonate	119		108	54	21
		95	67	38	24
Polyphenylene oxide			121	55	21
Polyetherimide	84		93	55	21
		99	38	37	24
Polysulfone			121	55	21
		86	64	48	24
PPO/Polystyrene (75/25)			206	61	21

adhesion to thermoplastics. Attempts were made to elucidate the reasons for the difference between these sets of fibers. Weak boundary layers and variations in surface roughness (as could be determined by equipment available to the investigators) were not the cause. Different levels of fiber surface treatment and various organic coatings also had no effect. Surface analysis of the fibers using XPS and retention time by inverse gas chromatography indicated a subtle difference in the surface chemical composition of the three fibers but the exact nature of these differences was not determined.[21] The acid-base characteristics of these fibers were measured with little difference between the two fiber types,[24] therefore some other mechanism, such as mechanical interlocking, may be controlling.

RESIDUAL COMPRESSIVE STRESSES

Because the usual thermoplastics do not contain groups capable of reacting with the fiber, covalent bonding of resin to fibers is precluded. One suggested mechanism is due to differential shrinkage from fabrication temperature to use temperature, p_T, as given by[25]

$$p_T = \frac{(\alpha_m - \alpha_f)\Delta T E_m}{(1 + \upsilon_m) + (1 - \upsilon_f)E_m/E_f} \tag{3}$$

where α is the linear coefficient of thermal expansion (CTE); ΔT, the temperature difference; E, the Young's modulus; υ, the Poisson's ratio; and subscripts f and m refer to fiber and matrix, respectively. There is a factor of 10 between the linear CTE of thermoplastic (CTE for ULTEM = 5.6×10^{-5}; for polysulfone = 5.5×10^{-5}) and the transverse value for carbon fibers (5.5×10^{-6}). While this mechanism surely is operable, it does not explain the differences observed between AS-4 and XAS in Table III. The various thermosets in Table III would have the same compressive forces on the two fiber types.

INVERSE GAS CHROMATOGRAPHY (IGC) AND ACID-BASE INTERACTIONS

The surface energy of a solid can also be determined by IGC, where the column packing is the item of interest and various vapors used as probe molecules. Some authors designate the polar part of the surface free energy as an acid-base interaction in order to be more quantitative on surface characterization. An acidic fiber surface should interact more strongly with a basic matrix and *vice versa*, hence the desire to characterize both fiber and matrix in these terms. For a non-polar liquid the retention volume of the probe molecule is related to the dispersive component of surface free energy of the fiber through

$$RT \ln V_n = 2N_A\{\gamma_S^D\}^{1/2} a\{\gamma_L^D\}^{1/2} + K_1 \tag{4}$$

where N_A is Avogadro's number; a, the surface area of the probe molecule; γ_L^D, the dispersive component of surface free energy of the probe liquid; γ_S^D, that of the substrate; and K_1, a constant depending on the reference state, the temperature, the surface area, and weight of fibers in the column.[26] By use of a series of non-polar hydrocarbons, γ_S^D can be evaluated. A schematic representation of Eq. (4) for a polar probe is shown in Figure 11 where ΔG_{SP}^O is the displacement of the polar probe value from that of an equivalent non-polar probe.[27] By measuring ΔG_{SP}^O at different temperatures, the specific enthalpy and entropy can be evaluated.

$$\Delta G_{SP}^O = RT \ln V_N / V_N^{\text{ref}} = \Delta H_{SP}^O - T\Delta S_{SP}^O \tag{5}$$

The exothermic term for acid-base interaction can be predicted with Gutmann's donor and acceptor numbers through

$$-\Delta H^{AB} = K_A[DN] + K_B[AN] \tag{6}$$

where ΔH^{AB} is set equal to ΔH_{SP}^O, $[DN]$ and $[AN]$ are Gutmann's numbers for probe molecules in IGC and K_A and K_B are numbers describing the acid and base characters of substate. The donor and acceptor numbers for some probe molecules are given in Table IV and the K_A and K_B values for some carbon fibers are given in Table V. The data in the upper part of Table V are from Elf-Aquitaine T-300 fibers: untreated, proprietary surface treated, the untreated fiber oxidized electrolytically in a laboratory pilot plant, oxidized T-300 with a proprietary sizing, and another commercially sized fiber[26]. The K_A's increase significantly on surface treatment but are not affected by the sizing. On the other hand, the K_B's are doubled on surface treatment and significantly

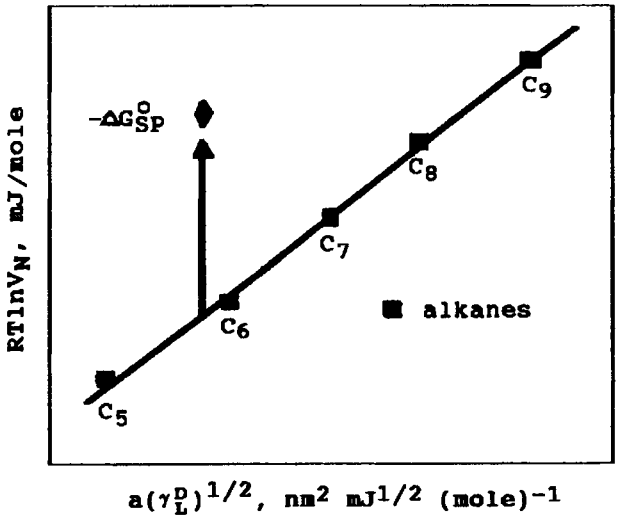

FIGURE 11 Determination of the specific free energy of desorption, $-\Delta G_{SP}^O$, of a polar probe molecule by inverse gas chromatography (Reprinted with permission from Lavielle and Schultz[27] © 1991 American Chemical Society).

TABLE IV
The surface area, a, of IGC probe molecules and the Gutmann donor [DN] and acceptor [AN] numbers (Reprinted with permission from Schultz and Lavielle[26] © 1989 American Chemical Society)

Probe	a nm^2	[DN]	[AN]
n-hexane	5.15	—	—
n-heptane	5.70	—	—
n-octane	6.28	—	—
n-nonane	6.89	—	—
carbon tetrachloride	4.6	0	8.6
chloroform	4.4	0	23.1
benzene	4.6	0.1	8.2
acetone	4.25	17.0	12.5
ethyl acetate	4.8	17.1	9.3
tetrahydrofuran	4.5	20.0	8.0
diethyl ether	4.7	19.2	3.9

TABLE V
Acid-base character of carbon fibers and matrices

Material	K_A kJ/mole	K_B kJ/mole
Data from Schultz and Lavielle[26] as corrected by Nardin *et al.*[28] (with $\pm$ symbol) along with Nardin *et al.* data.		
Untreated Soficar T-300	1.43 ± 0.12	1.5 ± 0.5
Oxidized T-300	2.22 ± 0.16	3.2 ± 0.2
Lab oxidized fiber	2.28 ± 0.16	3.6 ± 0.3
Coated & oxidized T-300	2.06 ± 0.16	13.0 ± 1.2
Coated T-300 washed with HCL	0.53	4.6
Coated T-300 washed with HCL + MEK	1.60	3.6
AS-4	0.60	9.8
A commercially coated fiber	2.14 ± 0.07	9.3 ± 0.3
Epoxy-1	1.79 ± 0.14	6.2 ± 0.5
Epoxy-2	2.37 ± 0.19	7.6 ± 0.6
PEEK	0.96	4.8
Calculated from Bolvari and Ward's data[24]		
Hercules AU-4	1.72	1.63
Hercules AS-4	2.42	2.04
Hysol Grafil XAS	2.19	2.11

increased by the coating. Additional data by this technique on sized fibers emphasizes the problems with the techniques used. The sized Soficar T-300 fibers were washed either with HCl or HCl followed by MEK (methyl ethyl ketone) to restore the fibers to the oxidized but noncoated condition. The values for the HCl washed fibers are quite different from the other T-300 fibers, indicating a more basic surface character. Washing the fibers with HCl and MEK essentially restored the K_A and K_B values to those of the oxidized fiber.[28] Note the different values between the upper and lower

parts of Table V for the AS-4 fiber (but certainly the samples were not obtained from the same lot number). The lower data in the table[24] were calculated from their ΔH values; the similarity of the acid-base character between AS-4 and XAS does not correlate with the differences in critical aspect ratios in thermoplastic polymers, Table III. Hence, acid-base character is also not the controlling parameter of adhesion of these two fibers to thermoplastics.

From a knowledge of the K_A and K_B values for fiber and matrix, a specific interaction parameter can be defined, A, describing the acid-base interaction between fiber and matrix:

$$K = K_A^f K_B^m + K_B^f K_A^m \tag{7}$$

On the other hand, the acid-base specific interaction parameter for fibers embedded in epoxy resins has a good correlation with IFSS, Figure 12, for the materials described in the upper part of Table V. The trends shown in Figure 12 are similar to those given in Figure 10, hence acid-base interaction is not the primary mechanism of adhesion.

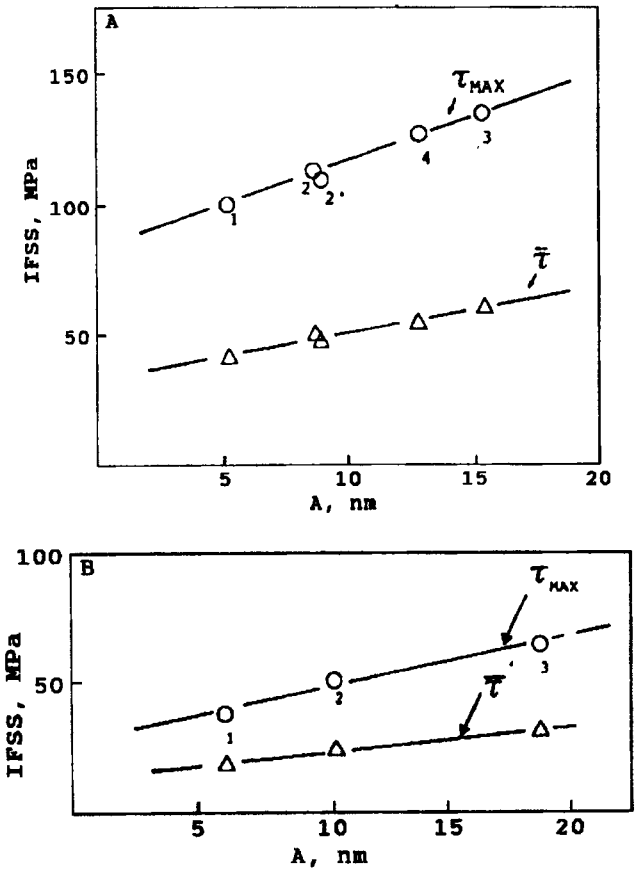

FIGURE 12 Correlation between IFSS by the fragmentation test and the acid-base specific interaction parameter A, Equation (7): (A) Epoxy-1; (B) Epoxy-2 (Reprinted with permission from schultz and Lavielle[26c] 1989 American Chemical Society).

EXISTENCE OF MICROROUGHNESS

The surface roughness of carbon fibers has been examined with the scanning electron microscope, which has a resolution down to about 50 nm. At this level of resolution, no evidence for roughening the surface was observed following surface treatment by various methods until treatment was severe enough to cause observable surface pitting. When pitting was observed, the fiber was sufficiently damaged to lower its tensile strength. Measurement of the surface areas of treated and untreated fibers show no change in surface area as determined by gas adsorption.

The scanning tunneling microscope (STM) functions on the basis of the quantum mechanical tunneling of electrons under the influence of a small bias voltage, ~25 nV, between an extremely sharp (ideally terminating in a single atom) metallic tip and a conducting surface separated by a gap of less than a nanometer. As the tip, Figure 13, is moved in three dimensions with an x, y, and z translator, it can trace the contours of the surface with atomic resolution (in the strict sense, the tip follows contours of constant electron density, hence the images contain both topographical and electronic information[29]). This high resolution is possible because the tunneling current is very sensitive to the distance between the tip and the surface. The current, 2–9 nA, typically can change by a factor of 2 due to a change in distance of 0.1 nm.[30]

Figure 14 shows a small graphitic region (4 nm × 4 nm) on an Amoco P-55 carbon fiber where the knobs indicate individual carbon atoms. The graphitic regions in P-55 are difficult to locate as they are interspersed with larger non-graphitic regions. The graphitic regions are far more prevalent in heat-treated MP fibers such as Amoco P-120[31]. At a larger scale (2000 nm × 2000 nm) Figure 15 shows the axial striations on P-55 that are readily observed in the SEM. In Figure 16 (9 nm × 9 nm), at about the

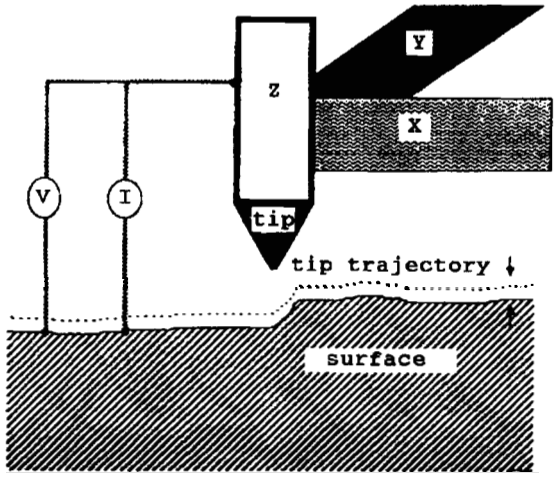

FIGURE 13 Schematic diagram of a scanning tunneling microscope showing the essential elements which include a sharp metallic tip connected to piezoelectric elements to control tip movement, an applied bias voltage and a measured tunneling current (Reprinted with permission from Hoffman *et al.*,[30] Figure 1,© Chapman & Hall, UK).

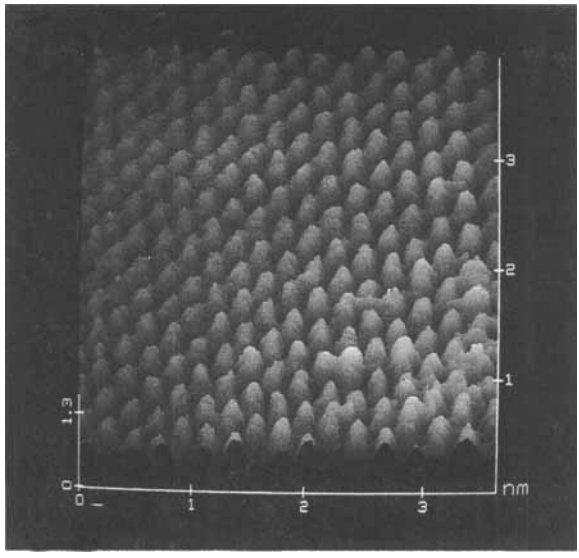

FIGURE 14 A scanning tunneling microscope (STM) image of Amoco P-55 carbon fiber showing a small graphitic region. Area is 4 nm × 4 nm. (Reprinted with permission from Hoffman *et al.*,[30] Figure 5,' Chapman & Hall, UK).

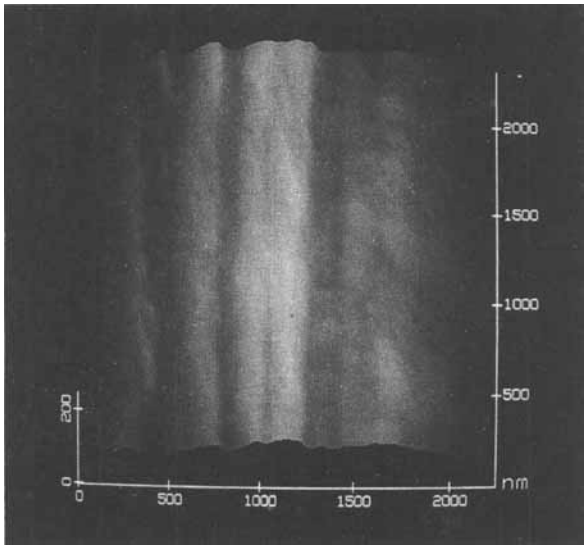

FIGURE 15 STM micrograph (2000 nm × 2000 nm) of Amoco P-55 fiber showing striations readily observed in the SEM (Reprinted with permission from Hoffman *et al.*,[30] Figure 3,© Chapman & Hall, UK).

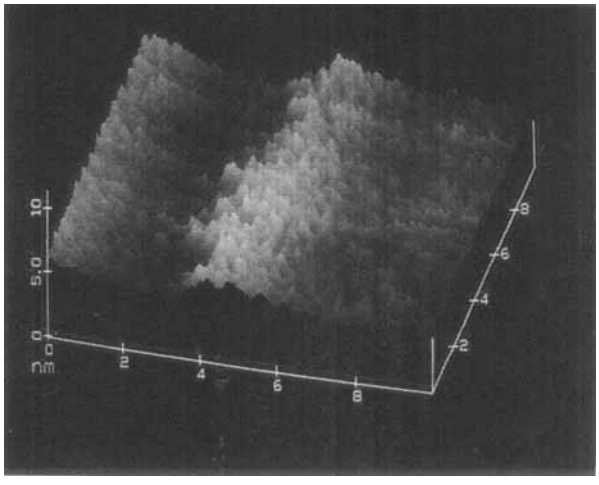

FIGURE 16 STM micrograph of an Amoco P-55 fiber surface treated in atomic oxygen to 0.66% weight loss at a scale of 9 nm × 9 nm exhibiting microroughness (Reprinted with permission from Hoffman *et al.*,[30] Figure 11,© Chapman & Hall, UK).

same scale as Figure 14 (4 nm × 4 nm), the surface shows an enhanced roughness after mild oxidation in an oxygen plasma. These differences cannot be observed in the SEM [29]. PAN-type carbon fibers show a different surface topography. Figure 17 show two views of sharp, jagged, and stepped surfaces of Amoco T-650/42 [31].

STM traces of the same series of IM-6 fibers shows increasing surface rugosity as surface treatment is increased from 20 to 600%[18]. Based on the increase in IFSS with

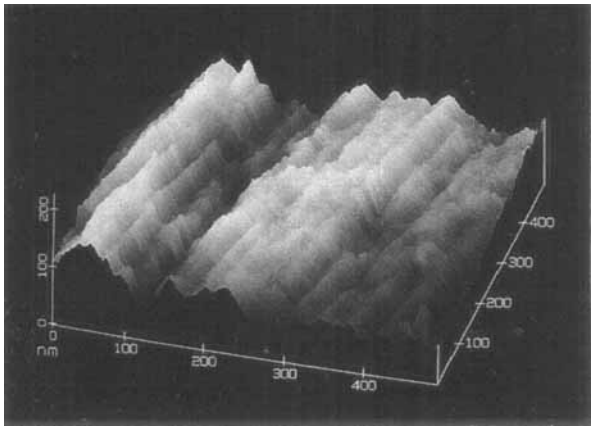

FIGURE 17 STM micrograph of an Amoco PAN-based fiber T-650/42 (A) scale 500 nm × 500 nm showing sharp and jagged edges,

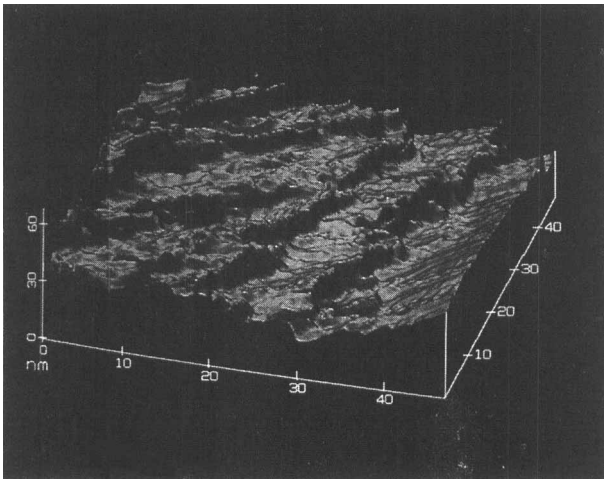

FIGURE 17 (*Continued*) (B) at a scale of 50 nm × 50 nm a stepped appearance results. (Hoffman *et al.*,[31] reprinted with permission from American Institute of Physics).

increasing surface treatment, the lowering of IFSS by blocking active groups with butyl glycidyl ether, and the increasing amount of microroughness in this series of IM-6 fibers, the conclusion is reached that 30% of the adhesion is due to chemical interaction and that mechanical interaction can be on the order of 50+%.[18]

Fiber microroughness could have two separate mechanisms of adhesion: the usual case of mechanical interlocking and modification of the stress fields near the fiber surface. The latter mechanism is based on the assumption that microroughness can be modelled as a series of connected planar surfaces. When load is applied, the stresses on each plane will depend on the orientation of that plane relative to the loading direction.[32] Thus, the stresses are distributed over a larger volume of material within the interphase than in the absence of microroughness. Far-field stresses would not be affected by microroughness.

CONCLUSIONS

To make durable adhesive bonds to aluminum or titanium, it is necessary to create a microrough surface into which the precursor molecules of the adhesive can penetrate. Figure 18 shows the micropore structure of aluminum after chromic acid anodization.[33] It may be that the critical need of carbon fibers to enhance bonding to thermoset and thermoplastic matrices is a microporous surface created by the surface treatment, and that the oxygen moieties are just an ancillary effect of creating the microporous surface. Indeed, as was shown earlier, reduction of the oxidized surface of a particular carbon fiber by hydrogen had only a small effect on the interfacial shear strength[13] plus the observation regarding the lowering of IFSS by prior reaction with butyl glydicyl ether. These observations indicate that mechanical interaction may be an important factor

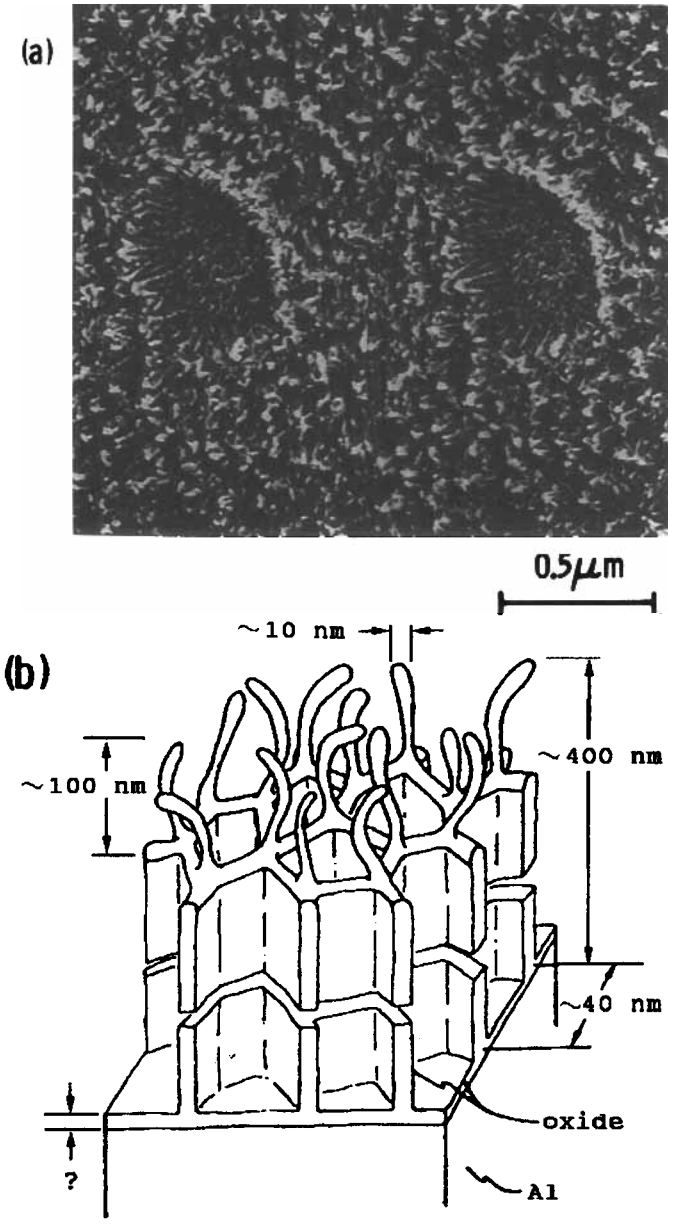

FIGURE 18 (a) Stereoscopic scanning transmission electron micrograph of an aluminum surface following chromic acid anodization, (b) schematic model of the aluminum oxide surface. (Venables *et al.*,[33] © Elsevier Science Publishers BV, Academic Publishing Division, reprinted with permission)

with covalent bonding, acid-base interactions and residual compressive stresses playing more minor roles. If mechanical interaction is the reason why XAS fiber bonds better to thermoplastics relative to AS-1 and AS-4 fibers, there must be a difference in the microroughness between these fiber types. To demonstrate whether mechanical

interactions through microroughness is indeed a dominant contributor to adhesion between carbon fibers and organic matrices, quantitative measures of microroughness are required. Such techniques are only now being developed. Measures based on fractal analysis may prove useful[34].

Acknowledgements

The author wishes to express his appreciation to Distinguished Alumni Professor J. P. Wightman of Virginia Tech for his contributions to the Science of Adhesion and the development of many adhesion scientists. He also appreciates the financial support of Dr. S. G. Fishman and the office of Naval Research as well as the many helpful comments on the manuscript by Mr. J. P. Armistead and Dr. A. S. Snow.

References

1. M. R. Piggott, *Composites Sci. Tech.* **42**, 57 (1991).
2. P. J. Herrera-Franco and L. T. Drzal, *Composites* **23**, 2 (1992).
3. L. H. Peebles, Jr., *Carbon Fibers: Formation, Structure and Properties* (CRC Press, Inc., Boca Raton, FL, 1994), in press.
4. B. D. Ratner, *Cardiovascular Pathology* **2**, No. 3 (Suppl.), 87S (1993).
5. S. S. Lin, US Army Materials Technology Laboratory Report MTL-TR-89–99, 1989.
6. Y. Nakayama, F. Soeda and A. Ishitani, *Carbon* **28**, 21 (1990).
7. T. Takahagi and A. Ishitani, *Carbon* **26**, 389 (1988).
8. T. A. DeVilbiss and J. P. Wightman, in *Composite Interfaces*, H. Ishida and J. L. Koenig, Eds. (North-Holland, New York 1986), p. 307.
9. D. Chan, M. A. Hozbor, E. Bayramli and R. L. Powell, *Carbon* **29**, 1091 (1991).
10. B. W. Chun, C. R. Davis, Q. He and R. R. Gustafson, *Carbon* **30**, 177 (1992)
11. J. Harvey, C. Kozlowski and P. M. A. Sherwood, *J. Mater. Sci.* **22**, 1585 (1987).
12. L. T. Drzal, M. Madhukar and M. C. Waterbury, *Composite Structures* **27**, 65–71 (1994).
13. L. T. Drzal, M. J. Rich and P. F. Lloyd, *J. Adhesion* **16**, 1 (1982).
14. P. Ehrberger and J.-B. Donnet, *Phil. Trans. Roy. Soc. London* **A294**, 495 (1980).
15. E. Fitzer and R. Weiss, *Carbon* **25**, 455 (1987).
16. E. Fitzer and R. Weiss, *Extended Abstracts, 16th Biennial Conf. on Carbon*, 1983, p. 473.
17. C. Kozlowski and P. M. A. Sherwood, *Carbon* **25**, 751 (1987).
18. L. T. Drzal, Adhesion Society Award Lecture, February 1994. to be published in *J. Adhesion*.
19. H. L. Cox, *Br. J. Appl. Phys.* **3**, 72 (1952).
20. W. W. Wright, *Composite Polymers* **3**, 231 (1990).
21. W. D. Bascom, K. J. Yon, R. M. Jensen and L. Cordner, *J. Adhesion* **34**, 79 (1991).
22. A. Kelly and W. R. Tyson, *J. Mech. Phys. Solids* **13**, 320 (1965).
23. M. J. Pitkethly, J. P. Favre, U. Gaur, J. Jakubowski, S. E. Mudrich, D. L. Caldwell, L. T. Drzal, M. Nardin, H. D. Wagner, L. DiLandro, A. Hampe, J. P. Armistead, M. Desaeger and I. Verpoest, *Composites Sci. & Tech.* **48**, 204 (1993).
24. A. E. Bolvari and T. C. Ward, *Inverse Gas Chromatography: Characterization of Polymers and other Materials*, ACS Sympos. Ser. **391**, D. R. Lloyd, T. C. Ward and H. Schreiber, Eds. (American Chemical Society, Washington, DC, 1989), p. 217.
25. L. DiLandro and M. Pegoraro, *J. Mater. Sci.* **22**, 1980 (1987).
26. J. Schultz and L. Lavielle, *Inverse Gas Chromatography*, ACS Symposium Series **391**, D. R. Lloyd, T. C. Ward and H. P. Schreiber, Eds., (American Chemical Society, Washington, DC, 1989), p. 185.
27. L. Lavielle and J. Schultz, *Langmuir* **7**, 978 (1991).
28. M. Nardin, E. M. Asloun and J. Schultz, in *Controlled Interphases in Composite Materials*, H. Ishida, Ed., (Elsevier, New York, 1990), p. 285.
29. W. P. Hoffman, *Carbon* **30**, 315, (1992).
30. W. P. Hoffman, W. C. Hurley, T. W. Owens and H. T. Phan, *J. Mater. Sci.* **26**, 4545 (1991).
31. W. P. Hoffman, W. C. Hurley, P. M. Liu and T. W. Owens, *J. Mater. Research* **6**, 1685 (1991).
32. L. H. Sharpe, *J. Adhesion* **6**, 15 (1974).

33. J. D. Venables, D. K. McNamara, J. M. Chen and T. S. Hopping, *Appl. Surf. Sci.* **3**, 88 (1979).
34. C. A. Brown, *Proc. 17th Annual Meeting of the Adhesion Society*, Orlando, FL, 1994, p. 5.
35. L. T. Drzal, M. J. Rich, M. F. Koenig, P. F. Lloyd, *J. Adhesion* **16**, 133 (1982).
36. L. T. Drzal, Private communication, 1991.

APPENDIX

The parameter σ_f, the tensile strength at the critical length l_c, is usually determined by extrapolation of log tensile strength against log gauge length. Values of σ_f for fibers listed in Table III are given in Table VI. The values of l_c were determined in different commercial DGEBA-type resins with different curing agents and curing procedures. Different XAS fibers were used in Tables III and IV (Hysol Grafil) and Table VI (Courtaulds). Despite these differences, the values of σ_f are sufficiently close to allow comparison of the critical aspect ratios between fibres.

TABLE VI
Values of σ_f for fibers listed in Table III

Fiber	σ_f GPa	Matrix	Ref
AS-1	4.51	1	35
AU-4	5.72	1	35
AU-4	5.83	1	35
XAS	5.24	2	36[3]

1: Epon 828 (Shell Chemical Co. a DGEBA-based resin), m-phenylene diamine (Aldrich Chemical Co.).
2: MY750 resin (Ciba-Geigy), NMA hardener, K61B curing agent (Ciba-Geigy).
3: Obtained by extrapolation of data provided in Reference 23 on Courtaulds XAS fiber.